Elsevier Editorial System(tm) for LWT - Food Science and Technology

Manuscript Draft

Manuscript Number: LWT-D-16-00494R2

Title: Effect of microwave power coupled with hot air drying on process efficiency and physico-chemical properties of a new dietary fibre ingredient obtained from orange peel

Article Type: Research paper

Keywords: microwave drying; energy consumption; citrus by-products; orange fibre; swelling capacity

Corresponding Author: Dr. Marta Castro-Giraldez, Ph.D.

Corresponding Author's Institution:

First Author: Clara Talens

Order of Authors: Clara Talens; Juan Carlos Arboleya; Marta Castro-Giraldez, Ph.D.; Pedro J. Fito

Abstract: Orange by-products are an excellent source of dietary fibre. The main objective of this work was to compare the physico-chemical and technological properties of fibres obtained from orange by-products by applying two different drying methods: hot air (HAD) and hot air coupled with microwave drying (HAD+MW). Process efficiency was also compared. 92 % reduction in processing time and 77 % reduction in energy consumption was achieved with HAD+MW. The drying treatment did not affect the physico-chemical properties of the fibres; however, the shrinkage-swelling phenomena that occurred during drying changed the rehydration properties of the fibre. HAD mainly affected the mechanical energy whereas HAD+MW affected the surface tension. An increase in particle size due to an increase in porosity during HAD+MW improved the fibre swelling capacity. HAD + MW can reduce drying time resulting in a more efficient drying process that positively affects the orange fibre's technological properties.

Effect of microwave power coupled with hot air drying on process efficiency and physico-chemical properties of a new dietary fibre ingredient obtained from orange peel

Clara Talens[a], Juan Carlos Arboleya[a], Marta Castro-Giraldez[b*], Pedro J. Fito[b]

[a]*AZTI - Food Research, Parque Tecnológico de Bizkaia, Astondo Bidea, Edificio 609, 48160, Derio (Bizkaia), Spain*

[b]*Instituto Universitario de Ingeniería de Alimentos para el Desarrollo, Universidad Politécnica de Valencia, Camino de Vera s/n, 46022 Valencia, Spain*

*author for correspondence: marcasgi@upv.es

Abstract

Orange by-products are an excellent source of dietary fibre. The main objective of this work was to compare the physico-chemical and technological properties of fibres obtained from orange by-products by applying two different drying methods: hot air (HAD) and hot air coupled with microwave drying (HAD+MW). Process efficiency was also compared. 92 % reduction in processing time and 77 % reduction in energy consumption was achieved with HAD+MW. The drying treatment did not affect the physico-chemical properties of the fibres; however, the shrinkage-swelling phenomena that occurred during drying changed the rehydration properties of the fibre. HAD mainly affected the mechanical energy whereas HAD+MW affected the surface tension. An increase in particle size due to an increase in porosity during HAD+MW improved the fibre swelling capacity. HAD + MW can reduce drying time resulting in a more efficient drying process that positively affects the orange fibre's technological properties.

Keywords: microwave drying, energy consumption, citrus by-products, orange fibre, swelling capacity

Abbreviations

MW	microwave drying
HAD	hot air drying
WRC	water retention capacity
TDF	total dietary fibre
IDF	insoluble dietary fibre
SDF	soluble dietary fibre
SC	swelling capacity
dm	dry matter
φ	relative humidity (-)
M	mass per time in wet basis (kg s^{-1})
M'	mass per time in dry basis (kg s^{-1})
x	mass fraction (kg kg^{-1})
X	absolute moisture (kg water kg dry air $^{-1}$)
t	time (s)
h	specific enthalpy (J kg^{-1})
p_s	water saturation pressure (kPa)
C_p	heat capacity at constant pressure (W g^{-1} K^{-1})
ΔH	molar enthalpy (J mol^{-1})

ρ	density (kg m^{-3})
v	velocity (m s^{-1})
S	section (m^2)
E	energy (kW or kWh)
W	microwave energy (W g^{-1})
P	absolute pressure (Pa)
T	temperature (K)
R	ideal gases universal constant (J mol^{-1} K^{-1})
Qc	isosteric heat
A	sample overall surface (m^2)
A^*	sample external surface (m^2)

Subscripts and superscripts:

amb	ambient conditions
da	dry air
D	drying conditions
0	initial time
v	vapour
w	water
i	internal

e	external
P	protein
F	fat
A	ash
C	carbohydrates
S	sugar
T	total
CEL	Cellulose
HEM	Hemicellulose
L	Lignin

1. Introduction

One important source of citrus dietary fiber is the residue generated by the orange juice industry (Fava et al., 2013; O'Shea, Arendt, & Gallagher, 2012). The ability to swell after water absorption is the principal physiological effect of fiber. The physico-chemical properties the fibre may be altered during processing operations such as drying (Bocco, Cuvelier, Richard, & Berset, 1998; García Herrera, Sánchez-Mata, & Cámara, 2010).

The main disadvantage of conventional hot air drying (HAD) is that it takes a long time, even at high temperatures, which in turn may cause serious damage to the product's quality attributes, such as flavour, colour, texture, nutrient status and beneficial health substances (Nijhuis, Torringa, Muresan, Yuksel, Leguijt, & Kloek, 1998; Tsami,

85 Krokida, & Drouzas, 1998). The application of coupled drying technologies such as hot
86 air-microwave drying (HAD+MW) could reduce the drying time and preserve the
87 quality of orange by-products (Fava et al., 2013; Talens, Castro-Giraldez, & Fito,
88 2016a). MW drying has achieved considerable attention in the recent past, gaining
89 popularity because of its advantages over conventional heating such as reducing the
90 drying time of biological material with small quality loss (Arslan & Ozcan, 2010;
91 Sahraoui, Vian, El Maataoui, Boutekedjiret, & Chemat, 2011). The theoretical basis of
92 drying treatments by hot air is to produce water fluxes from food sample to the air
93 stream induced by a gradient of water chemical potential (Demirel & Sandler, 2001).
94 The main drive of the water transport is the gradient between a_w and relative humidity
95 (Traffano-Schiffo, Castro-Giráldez, Fito, & Balaguer, 2014). A common technique is to
96 couple MW with hot air drying (Bergese, 2006; Kowalski, Rajewska, & Rybicki, 2005).
97 Talens, Castro-Giraldez, & Fito (2016b) reported a higher expansion phenomenon in
98 orange peels at 14 % water content after HAD+MW drying at 6 W/g compared to HAD.
99 One of the strategies used to improve the functionality of vegetable by-products is the
100 expansion of fibrous materials which in turn increases its specific surface area, thus
101 generating a greater retention of water (Bejar, Kechaou, & Mihoubi, 2011; Ghanem,
102 Mihoubi, Kechaou, & Mihoubi, 2012; Santana, 2009; Gu, Ruan, Chen, Wilcke, &
103 Addis, 2001; Lundberg, 2005; Ruiz-Díaz, Martínez-Monzó, Fito, & Chiralt, 2003;
104 Turbak, 1983).

105 The objective of this study was to compare the energy consumption of hot air drying
106 (HAD) *versus* hot air drying coupled with microwaves (HAD+MW) by analysing the
107 physico-chemical and technological properties of the dietary fibre obtained from orange
108 by-products.

109 **2. Materials and methods**

2.1. Fibre production process

Orange peels (Citrus sinensis (L.) Osbeck var Lane Late) were obtained after juice extraction by using a rotary press machine (Zumex Z450, Zumex Group, Valencia, Spain). Orange by-products were minced to 0.5 - 1 cm particle size using a cutter (Stephan UMC-5, Stephan, Germany) and blanched in water (ratio of 1 kg of fresh orange peel per 4 L of distilled water) at 65 ºC for 5 min. Afterwards, samples were centrifuged at 1 kg for 5 min using a high performance centrifugal machinery (Comteifa, Barcelona, Spain).

Blanched samples were treated in batches of 0.5 kg by two different drying methods in order to compare process efficiency and the physico-chemical and rheological characteristics of the fibre ingredient obtained. A pilot scale combined 2450 MHz electromagnetic MW and hot air drier equipment (MMP20T, Sairem S.A., Miribel, France) was used for HAD and HAD+MW treatments. Combined drying chamber dimensions were 0.66 m x 0.66 m x 0.83 m, air velocity was 7 m/s, hot air temperature was 55 ºC (relative humidity = 6.5 %), ambient temperature was 15 ºC and relative humidity was 60 %. For the energy consumption calculations, HAD, HAD+2 W/g, HAD+4 W/g and HAD+6 W/g were studied (the applied MW power was referred to the initial weight). The drying process was performed for each treatment until sample moisture was 0.01 kg_w/kg_T. Drying processes were stopped at different times in order to obtain the mass variation and moisture. Weight was measured by a precision balance Mettler Toledo AB304-S (± 0.001 g). Experiments were carried out in triplicate.

For physico-chemical analysis, samples treated by HAD and HAD+6 W/g were compared after 190 min and 15 min of drying, respectively. This was the time needed to reach 0.01 kg_w/kg_T of final moisture in orange by-product. After drying, samples were

134 milled using an ultracentrifuge mill (ZM 100, Retsch, Haan, Germany) with a sieve of
135 500 μm. At this stage, powder samples were sealed in plastic bags for further
136 characterization.

137 **2.2. Compositional analysis**

138 Powder samples were analysed according to the ISO recommended standards. Moisture
139 as in ISO 1442:1997 (ISO, 1997); ash as in ISO 936:1998 (ISO, 1998); protein content
140 was analysed by using the Digestion Unit K-435 and a distillation unit B-324 (Buchi
141 Labortechnik AG, Flawil, Switzerland). A correction factor of 6.25 was used as
142 recommended by ISO 937:1978 (ISO, 1978). Crude fat was analysed as in ISO
143 1443:1973 (ISO, 1973). Total sugars were analysed by Luff–Schoorl method for
144 reducing sugars (Lees, 1968). The carbohydrate content was determined by difference.

145 TDF, SDF, and IDF were determined by the AOAC enzymatic-gravimetric method,
146 991.43. Acid detergent fibre and acid detergent lignin was analysed by the gravimetric
147 method AOAC 973.18. Cellulose content was calculated as the difference between acid
148 detergent fibre and acid detergent lignin. Finally, hemicellulose content was determined
149 according to NF V 18-122 (AFNOR, 1997).

150 **2.3. Colour**

151 Colour was measured following CIELab scale. L*, a* and b* parameters were measured
152 using a Minolta CR-400 chromameter (Osaka, Japan), where L* is the parameter that
153 measures lightness, a* the tendency towards red and b* the tendency towards yellow.
154 The meter was calibrated using the standard white plate provided by the manufacturer
155 and powder samples were disposed over the whole surface of the plate for measurement
156 in triplicate.

2.4. Particle size distribution

Analysis of the particle size distribution was carried out using a laser diffractometer Mastersizer 2000 (Malvern Instruments Ltd, Malvern, UK) which has a particle size distribution range of 0.02 – 2000 μm. The Mie theory was applied by considering a refractive index of 1.5 and absorption of 0.01 (Park, 1995). The samples were analysed on laser diffraction with wet analysis using the Hydro S dispersion unit. Dry analysis was also performed using the Scirroco dry dispersion unit. Samples were diluted in de-ionised water at 2,000 rpm during 10 min. An obscuration rate of 15 % was obtained at each measurement. $D_{3,2}$ (surface weighted mean diameter) and $D_{4,3}$ (volume weighted mean diameter) were obtained.

2.5. Water retention and swelling capacity

Samples (0.5 g ± 0.0001 g) were hydrated in 20 mL of distilled water in a 50 mL falcon tube and left overnight to ensure the fibre was fully hydrated. Then, the tubes were centrifuged at 1000 × g for 10 min (adapted from Robertson, de Monredon, Dysseler, Guillon, Amado, & Thibault, 2000). The supernatant was decanted and the tubes were carefully inverted to drain residual unbound water from the sample. The remaining pellet was dried overnight in an oven at 105 ºC and weighed to consider possible solid matter losses in the draining step.

Swelling capacity (SC) was measured by the method of Raghavendra, Rastogi, Raghavarao, and Tharanathan (2004).

2.6. Rheology

In order to measure the rheological properties of the fibre, samples of fibre/water dispersion with a mass fraction of 0.06 kg_{Fibre}/kg_{T} were prepared. The rheological

180 characterization of the samples was carried out using a controlled-stress AR 2000
181 rheometer (TA Instruments, Leatherhead, United Kingdom). Stainless steel parallel
182 plate geometry of 40 mm diameter was used with a gap of 2 mm. A Peltier plate was
183 used to equilibrate and maintain the samples temperature at 20 ºC during the
184 measurements. A spoon was used to carefully load the sample on the bottom plate,
185 trying to minimize the structure breakdown. Samples rested for 2 minutes before any
186 determination was carried out to allow the stress induced during loading to relax.

187 Large and small deformation analyses were used for samples characterization. A flow
188 curve (large deformation) analysis was performed at increasing logarithmic shear rates,
189 from 0.001 to 100 s^{-1} to determine the viscosity of samples. Casson model was applied
190 to calculate the yield stress and the apparent viscosity of each sample (Lundberg, Pan,
191 White, Chau, & Hotchkiss, 2014). Dynamic oscillatory stress sweeps (small
192 deformation) were applied to investigate the viscoelastic behaviour of the samples with
193 a range of stress values from 0.1 to 2000 Pa at a constant frequency of 1 Hz. All the
194 measurements were carried out at least by triplicate.

195 **2.7. Microscopy**

196 Dehydrated particles were examined under a light microscope (DMLM Leica
197 Microsystems, Newcastle, UK) with a CCD camera incorporated which allowed
198 acquiring images for further analysis. Description of dehydrated samples was based on
199 examining sample surface variation each second over 40 s from dry until fully hydrated.
200 Subsequent treatment and measurement of the images was carried out by using Adobe
201 Photoshop v 7.0; Image J, 1.36 b free version. Measurements consisted on obtaining the
202 surface area of each sample. The response of particles to rehydration was assessed by
203 examining 5-10 particles per treatment.

204 **2.8. Statistical analysis**

205 To determine the statistical significance of the results an analysis of variance test
206 (ANOVA) was carried out with confidence levels of 95 % ($p \leq 0.05$) and 99 % ($p \leq$
207 0.01) using the program Statgraphics Plus 5.1.

208 **3. Results and discussion**

209 The basic composition of the citrus fibres obtained in this study is shown in Table 1.
210 There were no significant differences in water, protein, fat, ash, sugar or carbohydrates
211 contents among the fibres obtained by HAD or by HAD+MW. Due to the variability of
212 seasonality, cultivar, production process and region, these values can be considered
213 consistent with those reported by other authors (Chau & Huang, 2003; Lundberg et al.,
214 2014) for water (0.0742 ± 0.0073 kg_W/kg_T), protein (0.0815 ± 0.0045 kg_P/kg_T), fat
215 (0.0105 ± 0.0012 kg_F/kg_T), ash (0.0265 ± 0.0026 kg_A/kg_T), carbohydrates (0.8073 ±
216 0.0092 kg_C/kg_T) and sugar (0.0736 ± 0.0268 kg_S/kg_T) of commercial citrus fibre. TDF
217 was not significantly different among samples. The value obtained (0.61 ± 0.05
218 kg_{TDF}/kg_T for HAD and 0.59 ± 0.02 kg_{TDF}/kg_T for HAD+MW) was lower than that
219 reported by Lundberg et al. (2014) which was approximately 0.73 kg_{TDF}/kg_T. This might
220 be due to differences among cultivars as reported by Grigelmo-Miguel and Martín-
221 Belloso (1998).

222 The ratio of SDF:IDF obtained was 1:1, which means that the TDF was approximately
223 50 % soluble and 50 % insoluble in water. This ratio is higher for SDF than other
224 authors have reported in citrus fibre. Andrade, de Jong, and Henriques, (2014) reported
225 a ratio of SDF:IDF ranging from 1:1.2 to 1:1.4; and Grigelmo-Miguel and Martín-
226 Belloso (1998) obtained a ratio ranging from 1:1.7 to 1:2.2. This means that the fibre
227 obtained has a higher soluble to insoluble ratio, which can contribute to its suitability as

228 a food ingredient due to its ability for solubilisation in a food matrix. It is generally
229 accepted that fibre sources suitable for use as food ingredient should have an SDF:IDF
230 ratio close to 1:2 (Jaime, Molla, Fernández, Martín-Cabrejas, López-Andreu, &
231 Esteban, 2002; Schneeman, 1987).

232 Cellulose and hemicellulose contents were lower than those reported by Lundberg et al.,
233 (2014), 0.1595 ± 0.0002 kg_{CEL}/kg_T and 0.1006 ± 0.0015 kg_{HEM}/kg_T, respectively.
234 However, lignin content was higher than that estimated in another study carried out by
235 Grigelmo-Miguel and Martín-Belloso (1998) where the lignin content ranged from
236 0.022 – 0.03 kg_L/kg_T. These differences in fibre composition might be due to another
237 important factor: the ripening of the plant cells. The ripening is associated with a
238 gradual shift in fibre composition which is affected by the increase of cellulose and
239 lignin (McPherson, 1982). Differences in lignin content also might be due to the
240 method use for lignin determination. The acid detergent lignin method may account for
241 cutin and waxes which tend to remain in lignins (Van Soest, 1994), therefore, the lignin
242 content could be overestimated because it includes cutin and waxes.

243 Colour is another attribute that could be affected by temperatures reached during drying
244 (Table 2). No significant differences were found on lightness (L*) nor hue on a green (-)
245 to red (+) axis (a*) or either on b*, blue (-) to yellow (+) axis between HAD and
246 HAD+MW treatments. That showed that HAD+MW had the same effect as HAD on the
247 molecules responsible for colour in orange peels, such as β-carotene (Hecker, 2014).

248 Energy consumption was calculated as explained in Figure 1. The total energy required
249 for the HAD+MW process was calculated by adding the amount of energy required by
250 hot air (E_{HAD}) to the amount of energy required by MW (E_{MW}) per unit of time.

E_{HAD} was calculated by applying thermodynamics of humid air as explained in Green, and Perry (2007). If we consider the specific enthalpy (h) as the amount of heat (kJ/kg) used or released in a system at constant pressure, E_{HAD} could be calculated as the difference between the enthalpy of hot air at 55ºC (h_D) and the enthalpy of ambient air at 15ºC (h_{amb}) per kg of dry air (M'). The total energy consumption of microwaves was calculated as the total microwave power applied (W) per kg of wet product (M_0).

As air is a homogeneous mixture of dry air and water vapour, the enthalpy of hot air is found by taking the sum of the enthalpy of dry air and the enthalpy of water vapour in the humid air. The specific enthalpy of dry air is the total of the specific heat of dry air (Cp_{da}) multiplied by the temperature of drying (T_D). The enthalpy of water vapour depends on the specific heat of water vapour at a particular temperature (Cp_v), the absolute moisture (X) and the latent heat of vaporization (ΔH^v). The absolute moisture (kg_w/kg_{da}) is related to the partial pressure of water vapour. The partial pressure of water vapour is the total of relative humidity (φ) multiplied by the vapour pressure of saturated air at a specific temperature (p_s); the latter being dependent only on temperature. Thus, it is possible to obtain the vapour pressure of saturated air (ps_s^{amb} and p_s^D) at T_{amb} and $T_{D.}$

It was possible to calculate the specific enthalpy of ambient air and drying air (h_{amb} and h_D, respectively) by assuming that the absolute moisture of ambient air (X_{amb}) is equal to the absolute moisture of drying air at the beginning of the drying process (X_D^0). Finally, the mass of dry air (M') was calculated from the mass of humid air (M_D) and its absolute humidity (X_D^0). Also, M_D is a product of air density (ρ_D), air velocity (v_{air}) and the drier section (S_{Drier}). For air density estimation at 1 atm it was possible to apply the perfect gases law, therefore, ρ_D was calculated using φ_D and p_s^D. The relative

humidity of drying air (φ_D) is defined as the relationship between the partial pressure of water vapour and the vapour pressure of saturated air at $T_{D.}$ By using the relative humidity of drying air it was possible to calculate the partial pressure of water vapour as previously explained.

Table 3 showed that at higher microwave levels, the time needed to reach different moisture levels was significantly reduced. A strong time reduction was observed in all treatments by HAD+MW with regards to HAD at the initial stages of the drying (x_w = 0.5 kg_w/kg_T). After 122.5 min of drying by the HAD method a water content of 0.5 kg_w/kg_T was achieved, whereas only 9.6 min were needed drying by HAD+6 W/g to reach the same moisture content, which represents a 92 % reduction in time.

The process yield was 125 g fibre/ kg of fresh by-product. Figure 2 shows the energy required to achieve different reductions of moisture content by using HAD (0 W/g) or HAD+MW at different powers (2, 4 and 6 W/g). It is possible to observe how MW drying reduced energy consumption by up to 77 %. For instance, it was estimated that HAD would require 608.9 kWh in order to reduce the moisture content from 85 % to 10 % , whereas only 47.2 kWh were needed when using HAD+6 W/g.

HAD+MW drying involves simultaneous effects of the thermodynamics of hot air on the sample's surface, and the microwaves effect from the surface to the core, depending on the penetration depth of microwaves. The internal effect of microwaves produced mechanical and thermal phenomena which increased water mobility, and accelerated water transport thus reducing drying time. These phenomena were studied and published by Talens et al. (2016a) and Talens, Castro-Giráldez and Fito, (2016c) where a thermodynamic model was developed to explain and quantify the mechanisms involved in mass and energy transports throughout the combined drying of orange peels by HAD+MW and its microstructural effect.

In order to study the expansion effect of microwaves on the tissue of orange by-products, particle size distribution was measured in dried samples after milling. Table 4 shows the volume weighted diameter ($D_{4,3}$) and the surface weighted diameter ($D_{3,2}$) of orange peel powder samples dried by HAD and by HAD+6 W/g. It was observed that the $D_{4,3}$ of samples dried by HAD+6 W/g (466.5 ± 15.3 mm) were 30 % higher than the $D_{4,3}$ of samples dried by HAD (325 ± 8.7 mm). The same was observed with the surface weighted diameter $D_{3,2}$, which was 43 % higher ($p \leq 0.05$) for samples dried by HAD+6 W/g (260.1 ± 12.7 mm), than for samples dried by HAD (146.0 ± 5.8 mm). This could be explained due to the expansion phenomena that occurred during microwave drying, in which the samples swelled and increased their particle size. Talens, Castro-Giráldez, and Fito (2016b) showed a swelling in volume variation of orange peels treated by HAD+MW at different power intensities at both the macroscopic level and in micrographies.

Powdered samples were hydrated and the particle size was measured again (Table 4). Samples dried by HAD increased their $D_{4,3}$ by 1.76 times when hydrated, whereas samples dried by HAD + 6 W/g increase their $D_{4,3}$ by 1.37 times. $D_{3,2}$ increased 18 % in hydrated HAD samples whereas no increase $D_{3,2}$ was observed for hydrated HAD+MW samples.

Figure 3 shows the particle size distribution of dry and hydrated powder samples. It was observed that HAD+MW samples have higher percentage of larger particles both in dry and hydrated form.

WRC is the most common parameter used in the industry to characterize the rehydration capacity of fibre. It is also related to the physiological function of dietary fibre. Table 5

shows the results for the hydration properties measured. There were no significant differences in WRC (12.66 and 12.23 g_w/g_{dm}, respectively).

SC was significantly higher ($p \leq 0.01$) for HAD+MW samples (16.5 ± 0.7 mL/g_{dm}) compared to the HAD samples (14.75 ± 0.35 mL/g_{dm}). No differences were found in WRC among fibres obtained by different treatments, however, there were significant ($p \leq 0.05$) differences found in SC. Therefore, it can be concluded that HAD+MW caused an increase in particle size and porosity of orange powder samples which affected their SC but not their WRC.

Rheological characterisation of HAD and HAD+MW fibres was performed to study possible mechanical changes caused by the differences in both particle size and porosity. The flow behaviour of fibre dispersions presented non-newtonian shear-thinning behaviour, decreasing their viscosity with the application of increasing shear rates, which is in accordance with the typical behaviour of fibre suspensions. For this reason the experimental points could be adjusted to the Casson model, as it is commonly used to describe dispersions that have particles that interact in a pseudoplastic solvent (Lundberg et al., 2014). The parameters for Casson model (apparent viscosity and yield stress) are shown in Table 5. Although the apparent viscosity showed the same values for both types of fibre (Table 5), the shear stress that needs to be applied to the solution before it begins to flow (Yield Stress) was considerably higher in the case of HAD-treated fibre (165 Pa) compared to HAD+MW-treated fibre (88 Pa). This higher resistance to flow may be explained by the lower particle size of HAD-treated fibre (Table 4). At low shear rates, fibre molecules fuse to form an entangled network (Cepeda & Collado, 2014). At this point where entanglement occurs, the increase of viscosity with the concentration is much steeper.

347 The viscoelastic properties of both fibres were also investigated through oscillatory
348 measurements. Both samples presented a greater storage modulus (G') over the loss
349 modulus (G") confirmed by the low tan δ (G"/G') values along most of the oscillation
350 stress range (Figure 4). This behaviour indicates a predominant solid-like behaviour and
351 more precisely a gel-like structure (Sendra, Kuri, Fernandez-Lopez, Sayas-Barbera,
352 Navarro, & Perez-Alvarez, 2010).

353 HAD samples recorded higher G´and G" values compared to HAD+MW samples. As
354 explained above, the higher SC of HAD+MW fibre, made a weaker structure with
355 considerably lower storage modulus values.

356 In contrast, HAD fibre showed a stronger structure. This fact can be seen at higher
357 stresses when the structure is broken. The stress needed to collapse the system was
358 higher for HAD samples.

359 During rehydration, when fibre is in the glassy state with high mechanical energy stored
360 and high surface tension (Talens et al., 2016c), the gradient of the water's chemical
361 potential that causes the water to penetrate will be induced by the following equation:

362 $$d\mu_w = v_w dP + \sigma dA + RT \ln \frac{a_w^i}{a_w^e} \quad (1)$$

363 Where: $d\mu_w$ is the gradient of the water chemical potential, $v_w dP$ corresponds to the
364 mechanical term, σ is the surface tension, dA is the overall surface variation and a_w is
365 the water activity.

366 The two different drying techniques applied affect various terms of equation 1. HAD
367 mainly affects the mechanical term because higher mechanical energy is stored during
368 drying due to the shrinkage-swelling phenomena induced; therefore, more mechanical
369 energy of expansion was released during the rehydration. This phenomenon can be

observed in the micrographies (Figure 5a) throughout the samples rehydration, estimated as follows:

$$\Delta A^* = \frac{A_t^* - A_0^*}{A_0^*} \quad (2)$$

Where A^* the external surface of the sample, considering the bidimensional expansion of fibers, obtained from the micrographies, and subindexes: t is the time (1 s, 20 s and 40 s), and 0 is the initial time. In the evolution of external surface variation it is possible to observe the liberation of mechanical energy through the rehydration, being higher in HAD treatment. However, figure 5b shows the isosteric heat or adsorption energy, directly related with surface tension, indicating that the surface tension term is the most important contribution to the water chemical potential of HAD+MW samples. Therefore, the main contribution to the water chemical potential, during the rehydration process, is the mechanical expansion in case of HAD treatment and the surface adsorption in the HAD+MW treatment. The WRC (Figure 5b) is directly related with the water flux induced by the water chemical potential gradient, thus the contribution of the different treatments to the water chemical potential in fiber rehydration process, explained before, produces water fluxes with non significant differences; in conclusion, the fibers treated with HAD expand more but the fibers treated with HAD + MW retain more water for a same volume.

4. Conclusions

A new fibre ingredient was obtained from orange by-products by applying hot air coupled with microwave drying. An important reduction in processing time (92 %) and energy consumption (77 %) was achieved compared to hot air drying. The drying treatment did not affect chemical composition, water retention capacities or colour of orange fibres as compared to hot air drying. Total dietary fibre was close to 0.6

394 kg_{TDF}/kg_T with a ratio of SDF:IDF being 1:1. The shrinkage-swelling phenomena
395 occurred during drying affected the gradient of the water's chemical potential, changing
396 the rehydration properties of the fibre. An increase in particle size improved the fibre's
397 swelling capacity when hydrated.

398 **5. Acknowledgements**

399 The authors would like to acknowledge the Basque Government for the financial
400 support of the project (LasaiFood). The author Marta Castro-Giraldez wants to thanks to
401 the UPV Postdoctoral Program (PAID-10-14) from Universidad Politécnica de Valencia
402 for their support. The authors acknowledge the financial support from the Spanish
403 Ministerio de Economía, Industria y Competitividad, Programa Estatal de I+D+i
404 orientada a los Retos de la Sociedad AGL2016-80643-R. This paper is contribution nº
405 738 from AZTI (New Foods).

406 **6. References**

407 AFNOR. (1997). Association Française de Normalisation (AFNOR), 1997. Norme
408 Française homologuée, Aliments des animaux. Détermination séquentielle des
409 constituants pariéaux. Méthode par traitement aux détergents neutre et acide et à
410 l'acide sulfurique. *AFNOR, Paris, NF V 18–122*, 11.
411 Andrade, J. M. M., de Jong, E. V., & Henriques, A. T. (2014). Byproducts of orange
412 extraction: influence of different treatments in fiber composition and physical
413 and chemical parameters. *Brazilian Journal of Pharmaceutical Sciences*, *50*, 10.
414 Arslan, D., & Ozcan, M. M. (2010). Study the effect of sun, oven and microwave drying
415 on quality of onion slices. *LWT-Food Science and Technology*, *43*, 1121-1127.

Bejar, A. K., Kechaou, N., & Mihoubi, N. B. (2011). Effect of Microwave Treatment On Physical and Functional Properties of Orange (*Citrus Sinensis*) Peel and Leaves. *Journal of Food Processing & Technology*, *2*, 1-7.

Bergese, P. (2006). Specific heat, polarization and heat conduction in microwave heating systems: A nonequilibrium thermodynamic point of view. *Acta Materialia*, *54*, 1843-1849.

Bocco, A., Cuvelier, M.-E., Richard, H., & Berset, C. (1998). Antioxidant Activity and Phenolic Composition of Citrus Peel and Seed Extracts. *Journal of Agricultural and Food Chemistry*, *46*, 2123-2129.

Cepeda, E., & Collado, I. (2014). Rheology of tomato and wheat dietary fibers in water and in suspensions of pimento puree. *Journal of Food Engineering, 134*, 67-73.

Chau, C.-F., & Huang, Y.-L. (2003). Comparison of the Chemical Composition and Physicochemical Properties of Different Fibers Prepared from the Peel of *Citrus sinensis L. Cv. Liucheng*. *Journal of Agricultural and Food Chemistry*, *51*, 2615-2618.

Demirel, Y., & Sandler, S. I. (2001). Linear-nonequilibrium thermodynamics theory for coupled heat and mass transport. *International Journal of Heat and Mass Transfer*, *44*, 2439-2451.

Fava, F., Zanaroli, G., Vannini, L., Guerzoni, E., Bordoni, A., Viaggi, D., … Brendle, H.-G. (2013). New advances in the integrated management of food processing by-products in Europe: sustainable exploitation of fruit and cereal processing by-products with the production of new food products (NAMASTE EU). *New Biotechnology*, *30*, 647-655.

García Herrera, P., Sánchez-Mata, M. C., & Cámara, M. (2010). Nutritional characterization of tomato fiber as a useful ingredient for food industry. *Innovative Food Science & Emerging Technologies, 11*, 707-711.

Ghanem, N., Mihoubi, D., Kechaou, N., & Mihoubi, N. B. (2012). Microwave dehydration of three citrus peel cultivars: Effect on water and oil retention capacities, color, shrinkage and total phenols content. *Industrial Crops and Products, 40*, 167-177.

Green, D., & Perry, R. (2007). *Perry's Chemical Engineers' Handbook, Eighth Edition*: McGraw-Hill Education, New York, (Chapter 4, pp. 18-40).

Grigelmo-Miguel, N., & Martín-Belloso, O. (1998). Characterization of dietary fiber from orange juice extraction. *Food Research International, 31*, 355-361.

Gu, L., Ruan, R., Chen, P., Wilcke, W., & Addis, P. (2001). Structure-function relationships of Highly Refined Cellulose. *Transactions of the Asae, 44*, 1707-1712.

Hecker, S. (2014). *Extraction of β-carotene from orange peel and carrot waste for cotton dyeing*. Master in Science, Univerity of Boras, Sweden (pp. 22-33). Uploaded 26.06.14.

ISO. (1973). Determination of total fat content, ISO 1443:1973 standard *International standards meat and meat products*. Genève, Switzerland: International Organization for Standardization.

ISO. (1978). Determination of total nitrogen content, ISO 937:1978 standard *International standards meat and meat products*. Genève, Switzerland: International Organization for Standardization.

ISO. (1997). Determination of moisture content, ISO 1442:1997 standard *International standards meat and meat products*. Genève, Switzerland: International Organization for Standardization.

ISO. (1998). Determination of ash content, ISO 936:1998 standard *International standards meat and meat products*. Genève, Switzerland: International Organization for Standardization.

Jaime, L., Molla, E., Fernández, A., Martín-Cabrejas, M., López-Andreu, F., & Esteban, R. (2002). Structural carbohydrates differences and potential source of dietary fiber of onion (*Allium cepa L.*) tissues. *Journal of Agricultural and Food Chemistry, 50*, 122–128.

Kowalski, S. J., Rajewska, K., & Rybicki, A. (2005). Stresses generated during convective and microwave drying. *Drying Technology, 23*, 1875-1893.

Lees, R. (1968). *Laboratory handbook of methods of food analysis*. Leonard Hill Books, London, (pp. 118-124).

Lundberg, B. (2005). Using highly expanded citrus fiber to improve the quality and nutritional properties of foods. *Cereal Foods World, 50*, 248-252.

Lundberg, B., Pan, X., White, A., Chau, H., & Hotchkiss, A. (2014). Rheology and composition of citrus fiber. *Journal of Food Engineering, 125*, 97-104.

McPherson, K. (1982). Dietary fiber. *Journal of Lipid Research, 23*, 221-242.

Nijhuis, H. H., Torringa, H. M., Muresan, S., Yuksel, D., Leguijt, C., & Kloek, W. (1998). Approaches to improving the quality of dried fruit and vegetables. *Trends in Food Science & Technology, 9*, 13-20.

O'Shea, N., Arendt, E. K., & Gallagher, E. (2012). Dietary fibre and phytochemical characteristics of fruit and vegetable by-products and their recent applications as

novel ingredients in food products. *Innovative Food Science & Emerging Technologies, 16*, 1-10.

Park, J. W. (1995). Surimi Gel Colors as Affected by Moisture Content and Physical Conditions. *Journal of Food Science*, 60, 15-18.

Raghavendra, S. N., Rastogi, N. K., Raghavarao, K., & Tharanathan, R. N. (2004). Dietary fiber from coconut residue: effects of different treatments and particle size on the hydration properties. *European Food Research and Technology, 218*, 563-567.

Robertson, J. A., de Monredon, F. D., Dysseler, P., Guillon, F., Amado, R., & Thibault, J.-F. (2000). Hydration Properties of Dietary Fibre and Resistant Starch: a European Collaborative Study. *LWT-Food Science and Technology, 33*, 72-79.

Ruiz-Díaz, G., Martínez-Monzó, J., Fito, P., & Chiralt, A. (2003). Modelling of dehydration-rehydration of orange slices in combined microwave/air drying. *Innovative Food Science & Emerging Technologies, 4*, 203-209.

Sahraoui, N., Vian, M. A., El Maataoui, M., Boutekedjiret, C., & Chemat, F. (2011). Valorization of citrus by-products using Microwave Steam Distillation (MSD). *Innovative Food Science & Emerging Technologies, 12*, 163-170.

Santana, M. F. S., & Gasparetto, C. A. (2009). Microstructure of dietary fiber from orange albedo: a study by microscopy and physical techniques. *Ciência e Tecnologia de Alimentos, 29*, 124-134.

Schneeman, B. O. (1987). Soluble vs insoluble fiber – different physiological responses. *Food Technology, 47*, 81–82.

Selvendran, R. R. (1984). The plant-cell wall as a source of dietary fiber - chemistry and structure. *American Journal of Clinical Nutrition, 39*, 320-337.

Sendra, E., Kuri, V., Fernandez-Lopez, J., Sayas-Barbera, E., Navarro, C., & Perez-Alvarez, J. A. (2010). Viscoelastic properties of orange fiber enriched yogurt as a function of fiber dose, size and thermal treatment. *LWT-Food Science and Technology, 43*, 708-714.

Talens, C., Castro-Giraldez, M., & Fito, P. J. (2016a). A thermodynamic model for hot-air microwave drying of orange peel. *Journal of Food Engineering, 175*, 33-42.

Talens, C., Castro-Giraldez, M., & Fito, P.J. (2016b). Effect of microwave power coupled with hot air drying on sorption isotherms and microstructure of orange peel. *Food and Bioprocess Technology, in press.*

Talens, C., Castro-Giraldez, M., & Fito, P. J. (2016c). Study of the effect of microwave power coupled with hot air drying on orange peel by dielectric spectroscopy. *LWT - Food Science and Technology, 66*, 622-628.

Traffano-Schiffo, M. V., Castro-Giraldez, M., Fito, P. J., & Balaguer, N. (2014). Thermodynamic model of meat drying by infrarred thermography. *Journal of Food Engineering, 128*, 103-110.

Tsami, E., Krokida, M. K., & Drouzas, A. E. (1998). Effect of drying method on the sorption characteristics of model fruit powders. *Journal of Food Engineering, 38*, 381-392.

Turbak, A. F., Snyder, F.W., & Sandberg, K.R. (1983). Microfibrillated cellulose, a new cellulose product: properties, uses, and commercial potential. *Journal of the Applied Polymer Science, 37,* 818-827.

Van Soest, P. J. (1994). *Nutritional Ecology of the Ruminant.* (2th ed.). Cornell University Press, Ithaca, USA, (Chapter 12, pp. 187-188).

535 **FIGURE CAPTION**

536 Figure 1. Drying conditions and experimental data for calculating energy consumption
537 of two different drying processes applied to orange by-products: hot air drying (55 ºC)
538 and hot air combined with microwave drying at different power intensities (2, 4 and 6
539 W/g).

540 Figure 2. (a) Energy consumption (E_T in kWh) and (b) time consumption (t_D in min) for
541 drying orange by-products at different moisture contents (x_w in kg_w/kg_T) by applying
542 (●) hot air drying, (♦) hot air combined with microwave drying at 2 W/g, (▲) hot air
543 combined with microwave drying at 4 W/g and (●) hot air combined with microwave
544 drying at 6 W/g. Data represent means and standard deviation of experiments performed
545 in triplicate.

546 Figure 3. Particle size distribution of (———) hot air drying (dry fibre particles), (– –)
547 hot air drying (wet fibre particles), (———) hot air coupled with microwave at 6 W/g
548 (dry fibre particles) and (– –) hot air coupled with microwaves at 6 W/g (wet fibre
549 particles). Where: n_i = number of particles of one particular size, n_t = total number of
550 particles.

551 Figure 4. Representative stress sweep curves (elastic modulus G' and viscous modulus
552 G'') of a fibre/water dispersion (0.06 kg_F/kg_T) using fibres processed by two different
553 drying treatments: G' of fibre dried by hot air (———), G'' of fibre dried by hot air (
554 – –), G' of fibre dried by hot air coupled with microwaves at 6 W/g (———), G'' of
555 fibre dried by hot air coupled with microwaves at 6 W/g (– –). The lines are fits
556 using the Casson model.

557 Figure 5. (a) Top: micrographies of fibre particles dried by hot air (HAD) during the
558 rehydration process throughout time, where: t_0 refers to dried sample, t_1 refers to 1 s of
559 rehydration, t_{20} refers to 20 s of rehydration, and t_{40} refers to 40 s of rehydration.

Bottom: external surface variation (ΔA^*, dimensionless) with time of rehydration, where (●) is hot air drying and (●) is hot air drying coupled with microwaves at 6 W/g. (b) Top: micrographies of fibre particles dried by hot air coupled with microwaves at 6 W/g (HAD + 6 W/g) during the rehydration process throughout time, where: t_0 refers to dried sample, t_1 refers to 1 s of rehydration, t_{20} refers to 20 s of rehydration, and t_{40} refers to 40 s of rehydration. Bottom: table comparing isosteric heat (Qc) and water retention capacity of orange peel dried by hot air and by hot air coupled with microwave at 6 W/g.

Table

Table 1: Chemical composition (kg_i/kg_T) of the fibre obtained by hot air drying (HAD) and hot air coupled with microwave drying (HAD+ MW) of orange peel.

Composition (i) (kg_i/kg_T)	Orange fibre n = 3	
	HAD	HAD+MW
Water	0.0938 ± 0.0016	0.0977 ± 0.08
Protein	0.068 ± 0.005	0.068 ± 0.003
Fat	0.027 ± 0.003	0.021 ± 0.003
Ash	0.0326 ± 0.0012	0.034 ± 0.004
Carbohydrates	0.7874	0.7794
Sugar	0.1± 0.01	0.13± 0.03
TDF	0.61 ± 0.05	0.59 ± 0.02
SDF	0.30 ± 0.04	0.283 ± 0.013
IDF	0.31 ± 0.02	0.31 ± 0.02
SDF:IDF*	1:1	1:1
cellulose	0.092 ±0.012	0.112 ± 0.011
hemicellulose	0.07 ± 0.03	0.059 ± 0.012
lignin**	0.13 ± 0.02	0.110 ± 0.012

TDF (Total Dietary Fibre); IDF (Insoluble Dietary Fibre); SDF (Soluble Dietary Fibre); *SDF:IDF is the ratio between soluble and insoluble fibre and it is expressed as a relation. **Lignin is not a carbohydrate but it accounts for the insoluble part of dietary fibres. Data represent mean and standard deviation.

Table 2: Colour parameters (CIEL*a*b*) of orange fibres obtained by different drying methods: hot air drying (HAD) and hot air coupled with microwave drying (HAD + MW).

	HAD	HAD + MW
L*	77.50 ± 0.90	77± 1
a*	3± 1	3 ± 2
b*	66± 2	61± 4

Data represent mean and standard deviation, n = 3.

Table 3: Drying time needed for reaching 0.1, 0.2, 0.3, 0.4 and 0.5 water mass fraction (kg_w/kg_T) of orange by-products dried by hot air drying (HAD) and hot air drying coupled with microwaves (HAD+MW) at different powers (2, 4 and 6 W/g).

x_w (kg_w/kg_T)	time (min)			
	HAD	HAD+2 W/g	HAD+4 W/g	HAD+6 W/g
0.5	122.5	27.0	15.2	9.6
0.4	144.0	31.0	17.3	10.8
0.3	159.5	35.0	19.2	12.1
0.2	174.5	40.0	21.2	13.3
0.1	191.5	44.0	23.0	14.6

Table 4: Particle size distribution of the orange fibre obtained from orange by-products by applying hot air (HAD) and hot air coupled with microwave drying (HAD+MW).

	HAD		HAD + 6 MW	
particle size	dry	wet	dry	wet
$D_{4,3}$ (mm)	325 ± 9	572 ± 19	466 ± 15	642 ± 19
$D_{3,2}$ (mm)	146 ± 6	179 ± 9	260 ± 13	246 ± 16

$D_{4,3}$, $D_{3,2}$ represent volume weighted mean diameter, surface weighted mean diameter, respectively. Data represent means and standard deviation of experiments performed in triplicate (n=3).

Table 5: Physical properties of the fibre obtained by hot air drying (HAD) and hot air coupled with microwave drying (HAD + MW) of orange peel.

	Orange fibre	
	HAD	HAD + MW
WRC (kg_w/kg_{dm})	12.7 ± 0.5	12.2 ± 0.3
SC (mL/g_{dm})	14.8 ± 0.3	16.5 ± 0.7
Yield stress (Pa)*	165 ± 26	88 ± 27
Apparent viscosity (Pa/s)*	0.95 ± 0.19	0.91 ± 0.08

WRC (Water Retention Capacity), SC (Swelling Capacity).
*Values from Casson Model

Figure 1

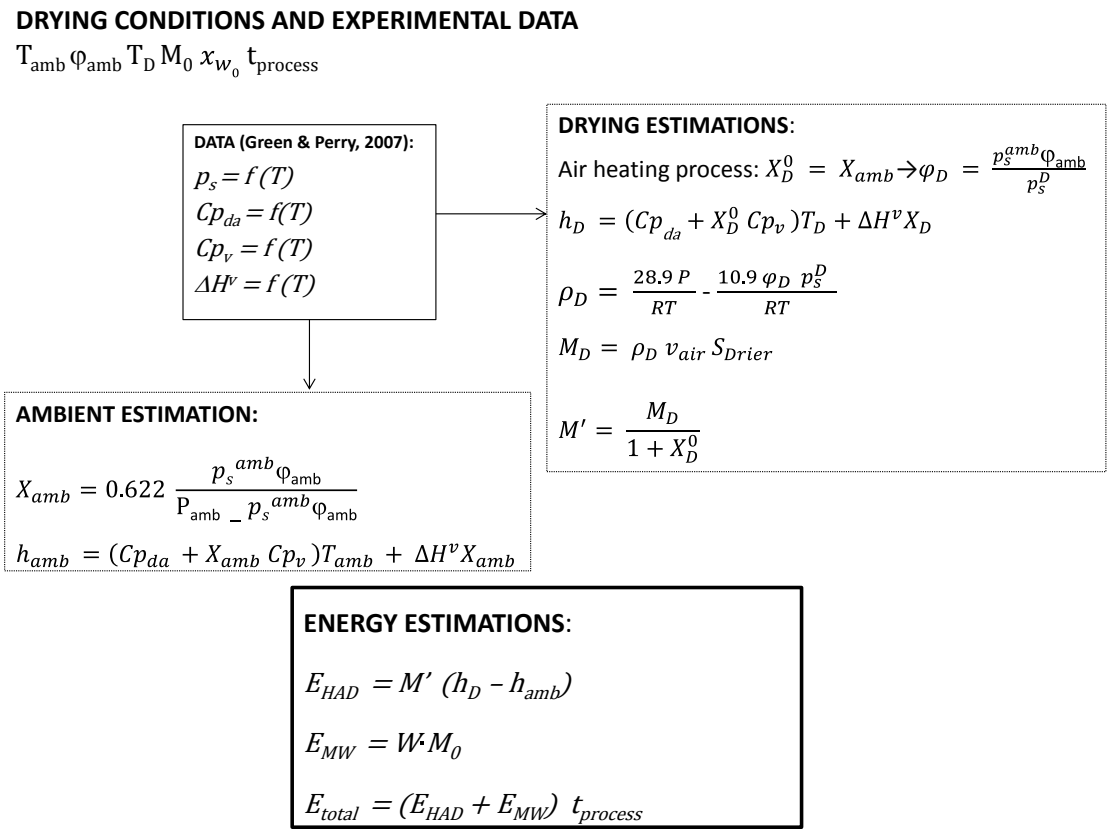

Figure 1

Figure 2

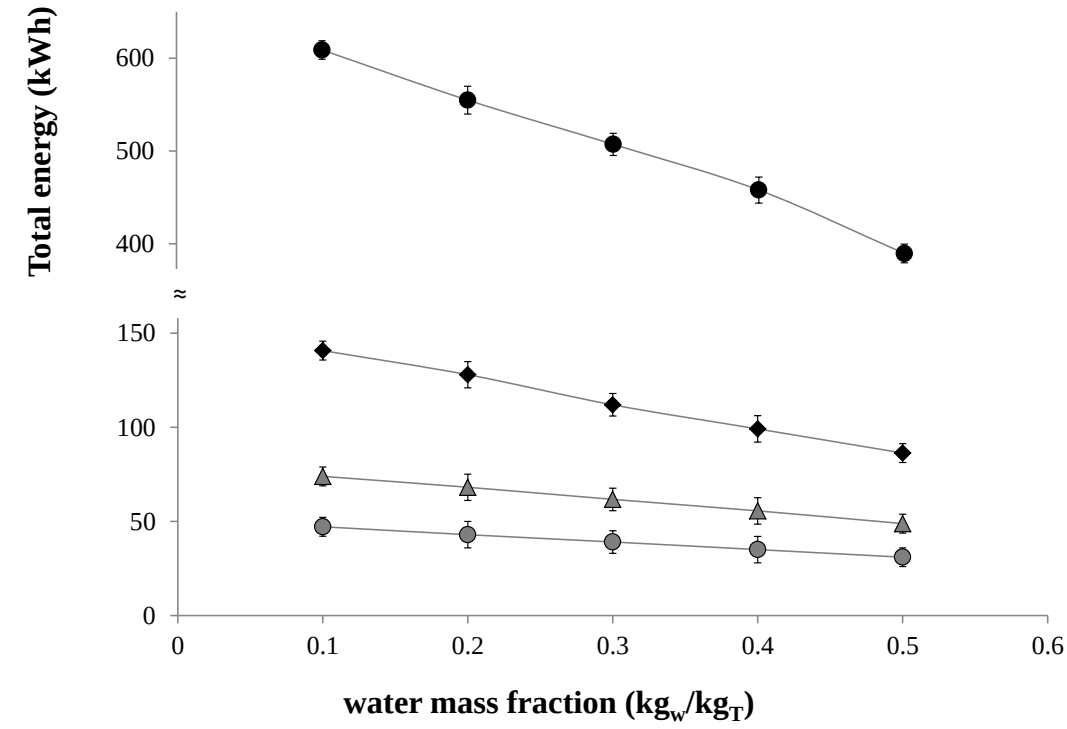

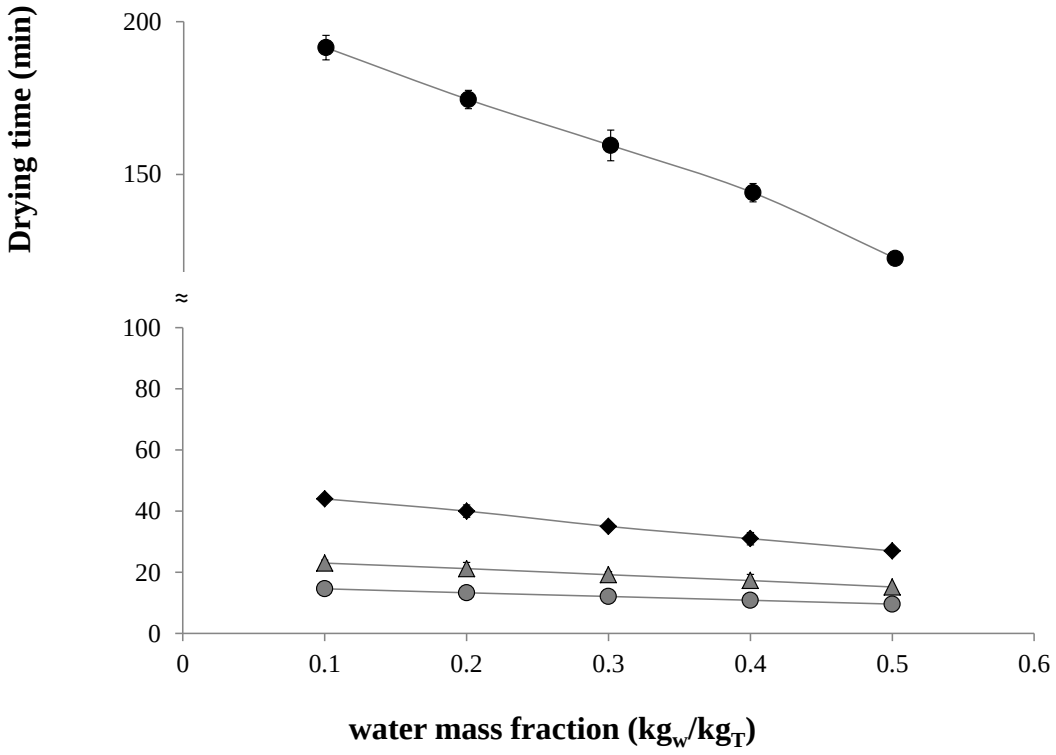

Figure 2

Figure 3

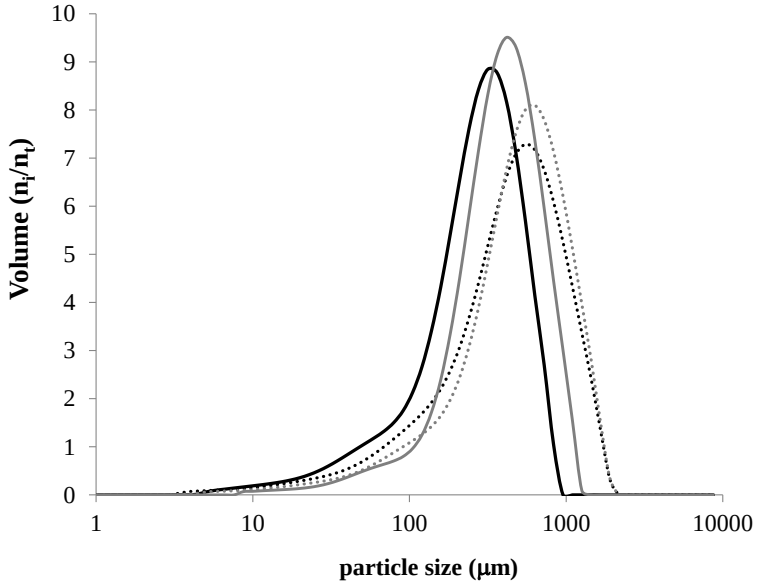

Figure 3

Figure 4

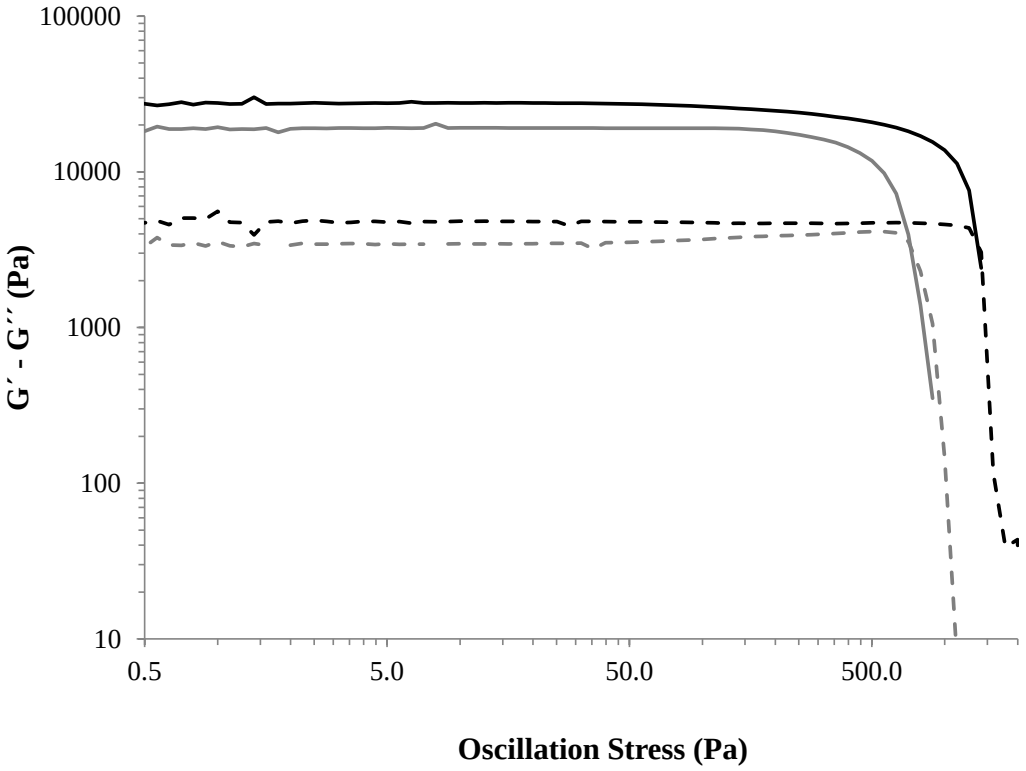

Figure 4

Figure 5

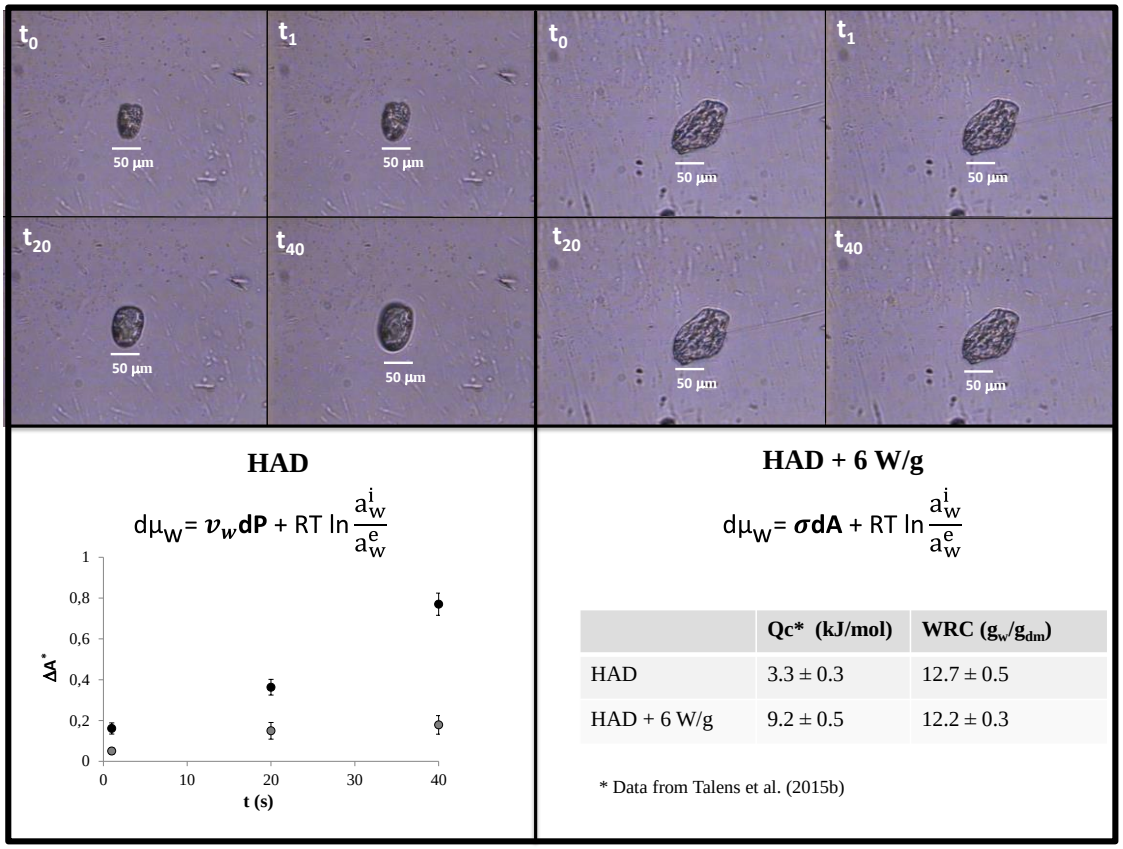

	Qc* (kJ/mol)	WRC (g_w/g_{dm})
HAD	3.3 ± 0.3	12.7 ± 0.5
HAD + 6 W/g	9.2 ± 0.5	12.2 ± 0.3

* Data from Talens et al. (2015b)

a) b)

Figure 5